International Journal of Progressive Sciences and Technologies (IJPSAT)
ISSN: 2509-0119.

http://ijpsat.ijsht-journals.org
Vol. 27 No. 2 July 2021, pp.441-454

The QSPR Studies of $[SO_4 (H_2O)_n]^{2-}$, n = 1–4, 16 Clusters through Quantum-Chemical Descriptors

Anant Babu Marahatta[1, 2]

[1]Department of Chemistry, Amrit Science Campus, Tribhuvan University, Kathmandu, Nepal

[2]Chemistry Subject Unit, Kathford International College of Engineering and Management (Affiliated to Tribhuvan University), Kathmandu, Nepal

Abstract – The quantitative structure property relationship (QSPR) is a powerful analytical approach that can link physicochemical properties of the molecular or ionic specimens mathematically with their 3D structures. The primary strategy of this predictive molecular based approach is to obtain optimum quantitative structure-property correlations by employing specific quantum-chemical descriptors (QCDs) that can encode structural features numerically. This theoretical insight is mainly aimed at computing HOMO and LUMO Eigen values and the associated QCDs such as HOMO-LUMO energy gap (ΔE_{gap}), Ionization potential (*IP*), Electron affinity (*EA*), Electronegativity (χ), Chemical hardness (η), Chemical softness (σ), Electronic chemical potentials (μ), and Electrophilicity index (ω) for the variably sized hydrated sulfate clusters $[SO_4 (H_2O)_n]^{2-}$, n = 1–4, & 16 separately using DFT:B3LYP hybrid functional, and predicting their most significant physical properties plus kinetic stabilities quantum mechanically. The major structure-based physical properties assessed here are electronic localization & polarizability, electronegativity, electrophilicity, degree of chemical hardness & softness, and the extent of global electron density transfer. The general results show that $[SO_4(H_2O)_4]^{2-}$ has more propensity to loose electrons among the ions with hydration number n < 4, and $[SO_4(H_2O)_{16}]^{2-}$ is the most kinetically instable ion having significant electronic polarizability among other smaller clusters sampled in this study. It is believed that this QCD based QSPR studies for the biologically most important and abundant micronutrient SO_4^{2-} ions would be highly useful to understand their physiological roles.

Keywords – Hydrated sulfate ions, Chemical stability, HOMO/LUMO, and QSPR analysis.

I. INTRODUCTION

In recent years, the fundamental principles of quantitative structure-activity and structure-property (hereafter, QSAR/QSPR) research approaches have been applied to different disciplines of science as they enable to predict most significant physicochemical properties and molecular activities from the concerned 3D molecular structures quantum mechanically [1], [2]. Due to this structure-property/activity correlations feature, these approaches are also used in finding out the most desirable and suitable molecular structures with unique and functionalized characteristics. The same feature actually makes them a quite short but very reliable searching route of the most promising chemical compounds for use in chemometrics, pharmacokinetics, pharmacodynamics, drug design and discovery, toxicology etc. [3]. However, a successful enquiry of this structure-activity/property interrelationships is not easy as expected. But, several advancements in the quantitative aspects of QSAR/QSPR have made them quite fascinating quantum mechanical approaches more especially in the field of modern chemistry, biochemistry, pharmaceutical science, and health research. For example, a direct employment of the quantum-chemical descriptors (hereafter, QCDs) derived from the properties of the molecules determined through quantum mechanical calculations in predicting meaningful structure activity/property interrelationships and molecular kinetic stability is one of the most widely used tools. In particular, the wisely

Corresponding Author: Anant Babu Marahatta

selected QCDs play significant roles in QSPR analysis as they speculate precise molecular physicochemical properties on the basis of which detailed insights into the nature of chemical compounds and their kinetic stability can be predicted.

In principle, the quantum-chemical descriptors are the most convincing and reliable source for describing almost all electronic and geometric properties of the molecules and their orbitals' interactions as they are formulated on the basis of quantum information of the molecular/ionic specimens mathematically [4], [5]. For instance, the descriptors E_{HOMO} and E_{LUMO} (energy of the highest (lowest) occupied (unoccupied) molecular orbital) provide quantitative information related to molecular/ionic stability and theoretical explanation related to electronic transitions plus approximate HOMO-LUMO energy gap ΔE_{gap} ($\Delta E_{gap} = E_{LUMO} - E_{HOMO}$, band gap) itself acts as a significant indicator to identify how intensely the molecules/ions take part in chemical reactions (smaller the ΔE_{gap}, faster is the electronic donation from HOMO to LUMO). In order to interpret QSPR analysis quantitatively, the E_{HOMO}, E_{LUMO} and ΔE_{gap} descriptors must be directly or indirectly used in the quantum mechanically formulated relationships (Eqs. 1–7) of few more important QCDs: Ionization potential (*IP*), Electron affinity (*EA*), Electronegativity (χ), Chemical hardness (η), and Electronic chemical potentials (μ) use them directly (Eqs.1–4, 6) while Chemical softness (σ) and Electrophilicity index (ω) use indirectly (Eqs. 5 & 7) [6], [7], [8], [9], [10], [11], [12].

$$IP = -E_{HOMO} \tag{1}$$

$$EA = -E_{LUMO} \tag{2}$$

$$\chi = \frac{(IP+EA)}{2} \tag{3}$$

$$\eta = \frac{(-E_{HOMO}+E_{LUMO})}{2} = \frac{\Delta E_{gap}}{2} \tag{4}$$

$$\sigma = \frac{1}{\eta} \tag{5}$$

$$\mu = -\frac{(I+EA)}{2} = -\chi \tag{6}$$

$$\omega = \frac{\mu^2}{2\eta} \tag{7}$$

In theoretical chemistry, several theoretical/computational methods that are either based on classical force fields or quantum-mechanical force fields are very often employed for optimizing low energy electronic structure and determining thermodynamic stabilities and dipole moments. But, only the molecular orbitals (MOs) based approach of quantum-chemical methods are used to compute E_{HOMO} and E_{LUMO} on the basis of which aforementioned electronic descriptors can be determined mathematically (Eqs. 1–7). The density functional theory (hereafter, DFT) is one of such approaches. Quantum mechanically, it is an LCAO-Kohn-Sham ansatz based theoretical model in relation with the spatially dependent electron density function [13], [14], [15]. It is known among the scientists as a quite efficient model having extraordinary abilities to cope with the complicated type quantum mechanical mathematical procedures in the limited computational resources (time and CPU memories) [13], [14]. It's remarkable skills in exploring ground state electronic structures of the many-body-multi-electron molecular/ionic systems and computing HOMO-LUMO interactions and E_{HOMO}, E_{LUMO} [15], [16], [17], [18], [19], [20], [21] side by side plus its wide applicability in quantizing those QCDs theoretically [22], [23], [24] are notable. Being DFT: B3LYP hybrid functional a successful method to predict a wide range of molecular properties, it is employed here to compute HOMO-LUMO Eigen values and ΔE_{gap} for the variably sized hydrated sulfate clusters $[SO_4(H_2O)_n]^{2-}$ n = 1–4 & 16 separately followed by the projection of their most important physicochemical properties on the basis of theoretically derived numerical indices of the QCDs. The triggering factors for conducting this quantum mechanical study on differently-sized hydrated sulfate clusters are to understand their experimentally observed: (1) water losing: $[SO_4(H_2O)n]^{2-} \rightarrow [SO_4(H_2O)n_{-1}]^{2-} + H_2O$; water gaining: $[SO_4(H_2O)n_{-1}]^{2-} + H_2O \rightarrow [SO_4(H_2O)n]^{2-}$; and charge separation: $[SO_4(H_2O)n]^{2-} \rightarrow [HSO_4(H_2O)n_{-k}]^{-} + [OH(H_2O)_{k-1}]^{-}$ reactions reported elsewhere [25], (2) electrons losing/gaining propensities in chemical reactions, (3) ability to firmly-hold electron cloud, (4) degree of chemical softness/hardness, and (5) electronic polarizability and electrophilicity more deeply. This sort of study for the hydrated sulfate ions may eventually provide important features that help to realize their physiological properties and roles in living organisms. Biologically, these ions are considered as the most important and abundant micronutrients in human tissues, cells, and plasma (300 μM). Most importantly, the influx and efflux mechanisms occurred in all the cells for the optimal supply of sulfate ions in the human body make these ions one of the

major sources of sulfur in many organisms [26]. Moreover, this study is useful to understand the variation in the physicochemical properties of the hydrated sulfate ions with respect to hydration number *n*, and their predominant activities in several sulfate-enriched aqueous systems such as electrolytes of flow battery systems [27], [28]; human body fluids [29], [30]; beverages such as beer, juice, milk, wine, mineral water etc.; foods and vegetables such as almonds, broccoli, bread, cauliflower etc.; laxatives (Na_2SO_4 solution) used for medical treatments etc. The structure of this paper is organized as: the computational details are outlined in section 2, the results and discussions are presented in section 3, and the conclusions are summarized in section 4.

II. COMPUTATIONAL DETAILS

Prior to calculate the numeral values of QCDs for the QSPR analysis of each and every hydrated sulfate $[SO_4(H_2O)_n]^{2-}$, n = 1–4 & 16, the most stable electronic structures of them (except for n = 16 cluster) were computed theoretically by using computationally designed molecular models as their trial structures. They were carefully built in *GaussView*: the Gaussian graphical interface [31], and the respective Cartesian coordinates of the atoms were extracted for geometry optimization. In the case of $[SO_4(H_2O)_{16}]^{2-}$ ion, the trial structure was directly displayed using Cartesian coordinates extracted from the database file produced through Monte Carlo simulation [32]. The concerned *Gaussian* keywords and methodologies were selected as instructed in *Gaussian* 09 manual [33]. The hybrid functional based DFT: B3LYP was employed with a greater basis set of the type 6–31G (*d*, *p*), where "6–31G" is the standard, split-valence double-zeta basis set: the mathematical functions that were used in the *Gaussian* script computationally while describing the core and valence orbitals of the atoms; and the functions inside parentheses "(*d*, *p*)" are polarization functions on heavy atoms and hydrogen for describing chemical bonds. Again, to direct *Gaussian* for running desirable computations, the ionic charge and spin multiplicity were specified as two integers in the format of (charge, spin multiplicity). Here, all the hydrated sulfate ions are anionic with similar negative charge units: $[SO_4(H_2O)_n]^{2-}$, n = 1–4 & 16 has charge units of −2 each with spin multiplicity 1. Hence, the set of integers used in their *Gaussian* input files were (−2, 1). Moreover, while solving electronic Schrodinger equation iteratively, the self-consistent field (hereafter, SCF) with both default SCF procedure (SCF=Tight) and Berny algorithm for geometry optimizations to a local minimum were selected [33], [34]. Since the current interest of the author is to understand QSPR of the differently sized hydrated sulfate clusters quantum mechanically, only the concerned QCDs (ionization potential (*IP*), electron affinity (*EA*), chemical hardness (η), chemical softness (σ), electronic chemical potentials (μ), electrophilicity index (ω), and electronegativity (χ)) are determined mathematically using DFT derived values of the E_{HOMO}, E_{LUMO}, and ΔE descriptors as formulated in equations (Eqs.1–7). While extracting these Eigen values, the *Gaussian* output files of each of these ions (such as *.log*, and *.fchk*) containing three dimensionally displayed chemical data were read by using *GaussView*, and the concerned molecular orbitals with HOMO–LUMO surface plots and Eigen values plus molecular electronic configurations were displayed in the 3D space.

III. RESULTS AND DISCUSSIONS

Even though the quantum mechanically derived descriptors (*IP*, *EA*, η, σ, μ, ω, and χ) are incapable of addressing the bulk effects directly [35], the quantitatively determined magnitudes of them in QSPR studies can reveal successful structure property correlations. As there is mostly no any internal error in the computational process except the minor assumptions made while formulating the concerned quantum mechanical model efficiently, the process of elucidating structure activity/property relations on the basis of fundamental principle of the quantum chemistry-based descriptors is more reliable than those predicted by experimentally measured descriptors [35]. According to quantum mechanical theory, these descriptors have direct relations with the Eigen values E of only those molecular orbitals (MOs) that are most spatially delocalized at the frontier part of the molecules/ions: HOMO and LUMO. Apart from this, these orbitals and their interactions play significant roles in determining chemical stability of any molecular specimens, and their subsequent analysis provides primary information for explaining intramolecular HOMO–LUMO charge transfer phenomena and the related consequences. Additionally, incorporating HOMO–LUMO orbital interactions with their energy gap (ΔE_{gap}) mathematically provides quantitative explanation for predicting kinetic stability of any types of the molecular/ionic compounds including their degree of hardness, softness (concept of hard and soft nuleophiles and electrophiles) and electronic polarizabilities. The DFT computed surface plots of these orbitals depicting concerned HOMO–LUMO energy gaps (ΔE_{gap}) for the variably sized hydrated sulfate ion clusters $[SO_4(H_2O)_n]^{2-}$, n = 1–4 &16 and their quantum mechanical relations with the reactivity descriptors are separately discussed below.

3.1 HOMO–LUMO gap (ΔE_{gap}) in predicting kinetic stability

In order to estimate the wide-range of quantum mechanical descriptors quantitatively for QSPR analysis of the variably sized hydrated sulfate ions $[SO_4(H_2O)_n]^{2-}$, n = 1–4 & 16, the required HOMO-LUMO surface plots, and their Eigen values E_{HOMO} and E_{LUMO} are extracted from the DFT generated quantum mechanical information and are displayed in Figure 1 to Figure 5, where the calculated values of their energy gap ΔE_1, ΔE_2, ΔE_3, ΔE_4,and ΔE_5 in both *Hartree* (*a.u.*) and electron volt (eV) units are clearly mentioned. As one can see in each of these figures, the electron density surfaces of the HOMO are distributed mainly over the central SO_4^{2-} (highly localized) units while the LUMO surfaces show a significant probability electron density over the hydrated surrounding H_2O molecules. This variation of the electronic occupancy in the frontier molecular orbitals has not only outlined the possibility of undergoing electronic delocalization from the central SO_4^{2-} unit to surrounding H_2O molecules in the course of structural stabilization as reported elsewhere [20] by the same author but also verified the optical excitation (HOMO to LUMO transition) phenomena shown by the HOMO electron. Appearance of the holes on the LUMO surfaces of all the hydrated sulfate ions sampled in this study further demonstrates the origination of attractive force that can bind electron cloud more closely to the ionic centers. Moreover, the DFT derived HOMO-LUMO energy gaps $\Delta E_1 = 8.98\, eV, \Delta E_2 = 8.93\, eV, \Delta E_3 = 8.56\, eV$, $\Delta E_4 = 8.54\, eV$, and $\Delta E_5 = 3.05\, eV$ for the $[SO_4(H_2O)_n]^{2-}$, n = 1–4 & 16 ions respectively not only approximates their band gaps (electronic band gaps) exist in between valence band and conductance band but also predicts individual lowest energy transition frequency in UV visible spectroscopy. While comparing these values to each other, the trend is in decreasing order: $\Delta E_1 > \Delta E_2 > \Delta E_3 > \Delta E_4 > \Delta E_5$with increasing hydration number n of the SO_4^{2-} ion. It ascertains that the HOMO to LUMO electronic transition takes place comparatively more easily with increasing hydration number n, suggesting bigger clusters are kinetically less stable (larger ΔE_{gap} always infers higher ionic/molecular stability means lower is the chemical reactivity) even though they are thermodynamically/energetically more stable as predicted by electronic structure calculations [20]. For example, among the sulfate ion hydrated clusters with n = 1–4 & 16, the

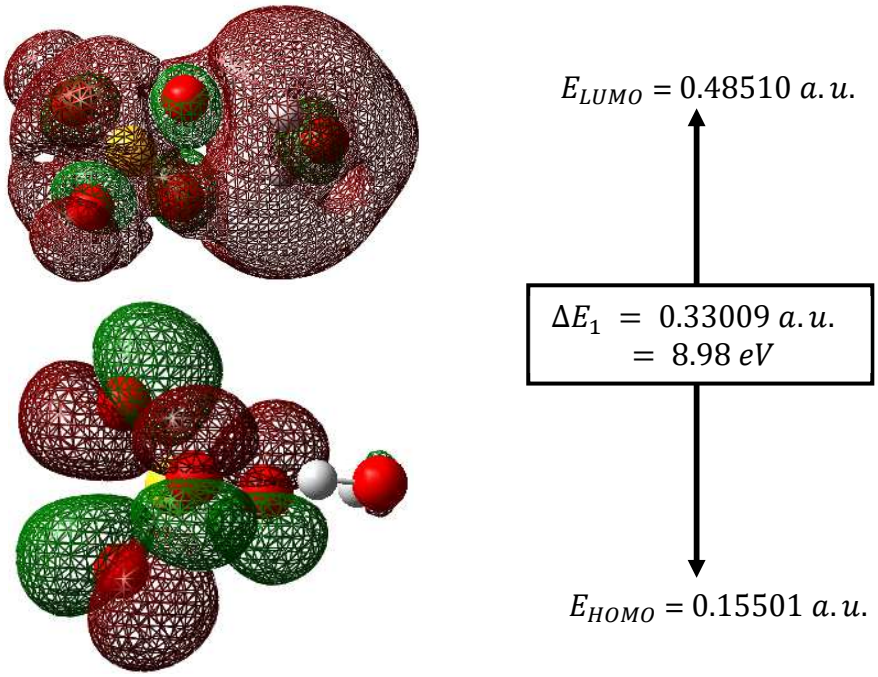

Figure 1. DFT computed surface plots of HOMO and LUMO depicting HOMO–LUMO energy gap ΔE_1 for $[SO_4(H_2O)]^{2-}$ ion.

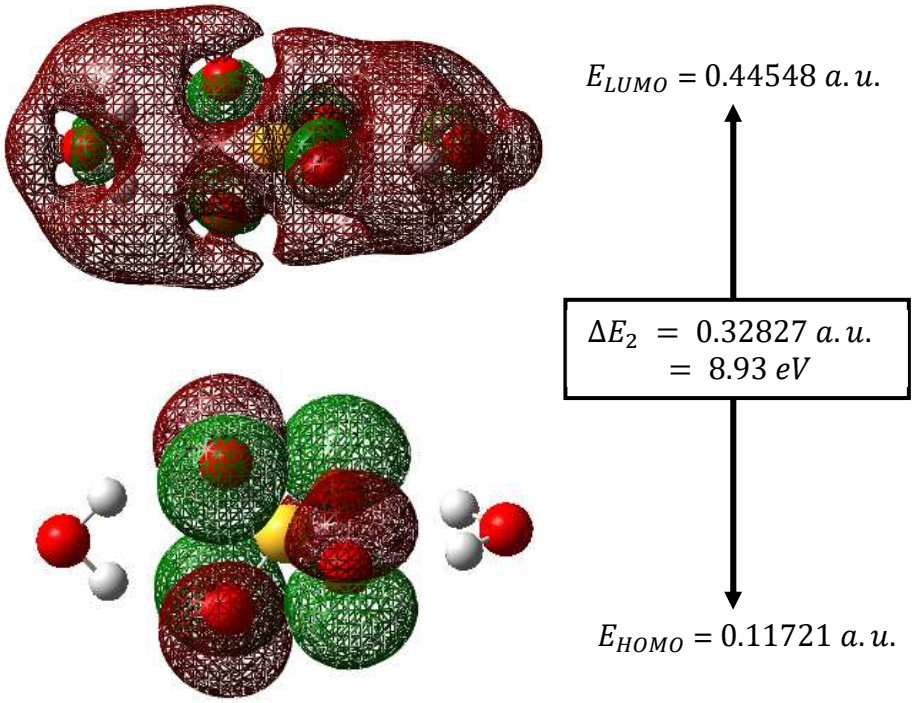

Figure 2. DFT computed surface plots of HOMO and LUMO depicting HOMO–LUMO energy gap ΔE_2 for $[SO_4(H_2O)_2]^{2-}$ ion.

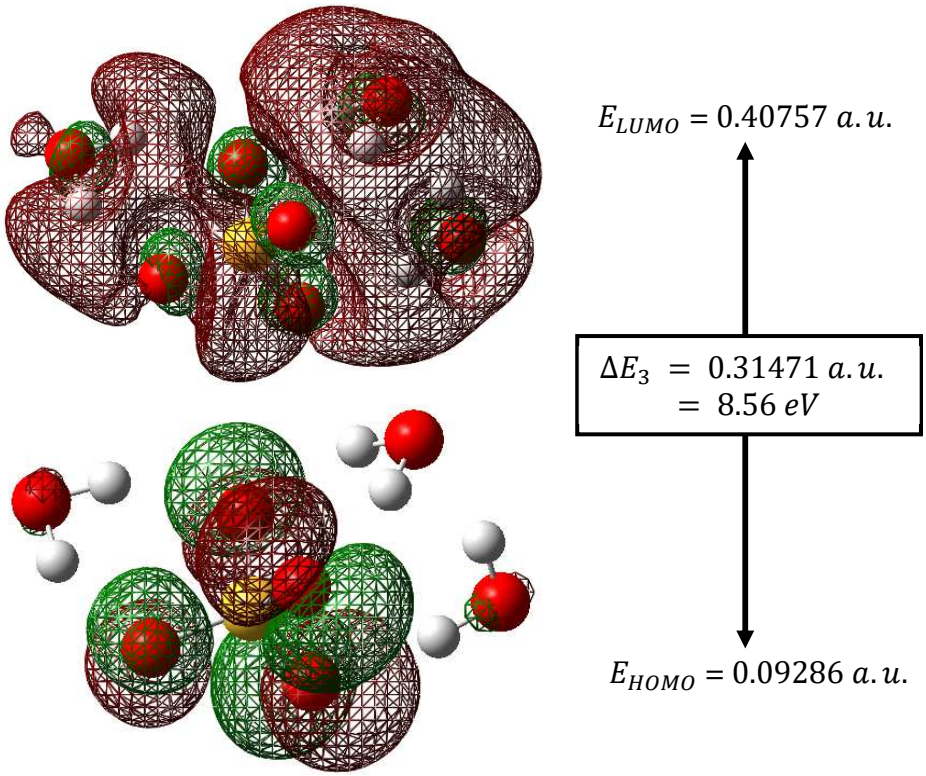

Figure 3. DFT computed surface plots of HOMO and LUMO depicting HOMO–LUMO energy gap ΔE_3 for $[SO_4(H_2O)_3]^{2-}$ ion.

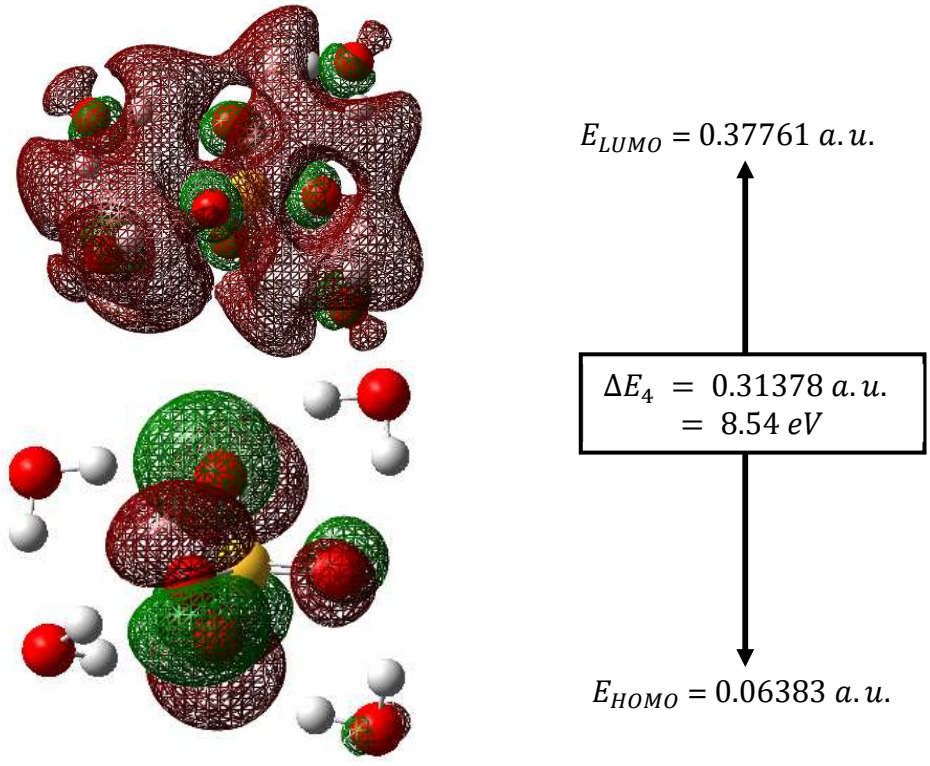

Figure 4. DFT computed surface plots of HOMO and LUMO depicting HOMO–LUMO energy gap ΔE_4 for $[SO_4(H_2O)_4]^{2-}$ ion.

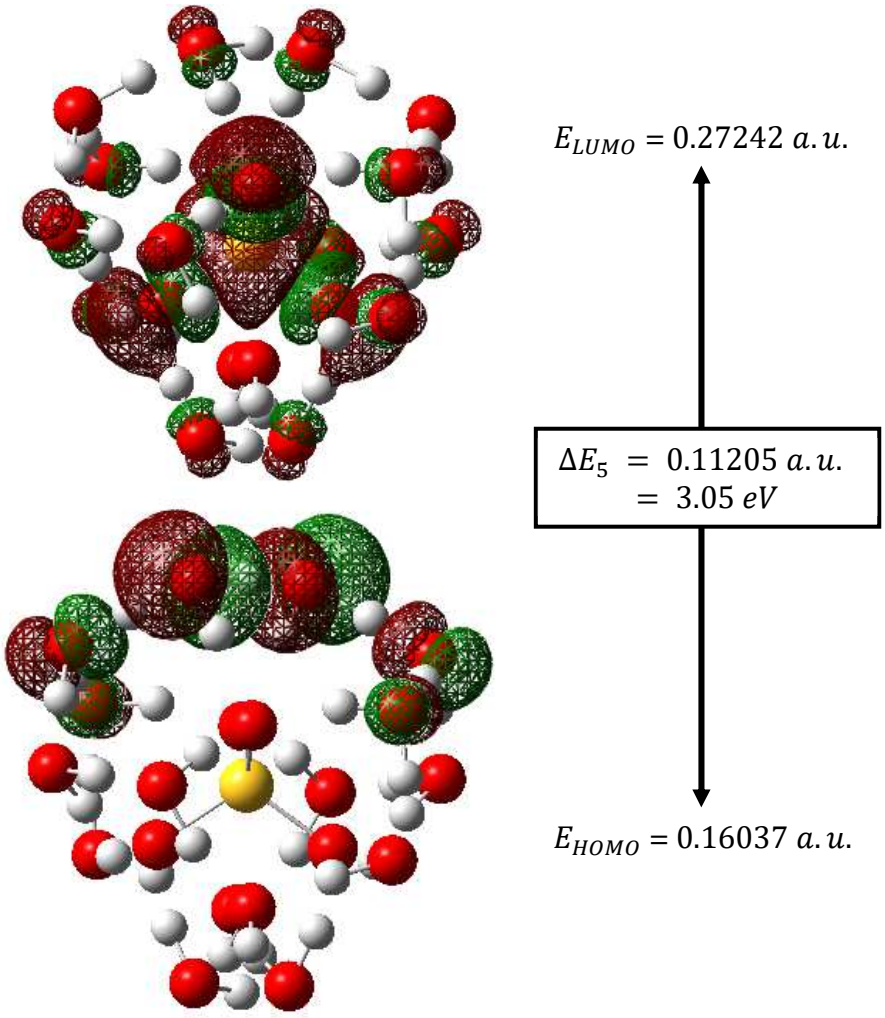

Figure 5. DFT computed surface plots of HOMO and LUMO depicting HOMO–LUMO energy gap ΔE_5 for $[SO_4(H_2O)_{16}]^{2-}$ ion.

easiest HOMO to LUMO electronic transitions occurs in the cluster with n = 16: $[SO_4(H_2O)_{16}]^{2-}$, implying that it is kinetically the least stable (more reactive) cluster. In particular, the band gap ΔE_1 for the cluster $[SO_4(H_2O)]^{2-}$ (n = 1) is as equal as the band gap ΔE_2 for $[SO_4(H_2O)_2]^{2-}$ (n = 2), and the band gap ΔE_3 for the cluster $[SO_4(H_2O)_3]^{2-}$ (n = 3) is again as equal as the band gap ΔE_4 for $[SO_4(H_2O)_4]^{2-}$ (n = 4). It further means that the paired or unpaired electron present in the HOMO of the first ion (n = 1) undergoes as fast transition as in second ion (n = 2), and the same is the case in between third (n = 3) and fourth (n = 4) ion. But, the rate of optical electronic transition that takes place from HOMO to LUMO in the clusters $[SO_4(H_2O)]^{2-}$ and $[SO_4(H_2O)_2]^{2-}$ must be slower than that occurring in both $[SO_4(H_2O)_3]^{2-}$ and $[SO_4(H_2O)_4]^{2-}$ clusters. Again, the relatively smaller band gap ΔE_5 for the $[SO_4(H_2O)_{16}]^{2-}$ hydrated state signifies an occurrence of the fastest electrons/charges migration from HOMO to LUMO, eventually clarifying how the energy transfer events are intensified or the ionic type chemical reactions are initiated (HOMO electrons are very often considered as the most reactive). The detailed structure based properties (QSPR) for these variably sized hydrated sulfate ion clusters can only be predicted after analyzing the quantum mechanically determined numerical QCDs as explained below logically and concisely.

3.2. Quantum-chemical descriptors (QCDs) in QSPR analysis

In QSPR studies, many good quantum-chemical (mechanical) descriptors are used to represent significant molecular features and to reflect simple molecular properties numerically. They are actually called global numerical indicators due to their importance and responsibility in providing quantum mechanical insights into the most appropriate molecular/ionic properties which in turn are

highly associated with their structure based activities (QSAR) [36]. In this section, a brief explanation of the concerned molecular descriptors and their remarkable significance in featuring structure property/activity correlations are presented in reference to the variably sized hydrated sulfate ion clusters $[SO_4(H_2O)_n]^{2-}$, n = 1–4 & 16.

3.2.1 Ionization Potential (*IP*), Electron Affinity (*EA*), and Electronegativity (χ)

Ionization potential (*IP*) of any molecular or ionic specimen is such type of the parameters used in QSPR analysis that can measure binding force of the electrons themselves are held centrally through the positively charged nucleus [37], [38]. As it approximates the amount of energy required (endothermic type energy) to remove most loosely bound electron out of the nuclear province from the isolated molecular or ionic specimens in their ground electronic state, the absolute magnitude of it can be used to work out on the strength of the chemical bonds as well. More importantly, the quantum mechanically derived absolute value of it can be used as a descriptor to predict kinetic stability of the molecular or ionic specimens. It is based on the fact that molecules or ions having less-tightly held electrons must have comparatively low *IP* values and hence, they have high tendency of acting as good reducing agents (high propensity of losing electrons or undergoing oxidation) and generating corresponding cationic forms more likely. It eventually infers that such molecules or ions are comparatively more reactive, less kinetically-stable/chemically-inert and have high susceptibility towards electrophilic attack. Unlike *IP*, another QSPR descriptor "Electron Affinity" (*EA*) is defined by an energy released (exothermic type) while adding an extra electron to the atom of isolated molecules/ions in the ground state [38]. In other words, it evaluates the intensity of gaining an electron by the isolated ionic or molecular specimens. The DFT derived absolute value of this quantum mechanical indicator is very often used to predict oxidizing/reducing properties of the molecules/ions and to characterize their susceptibility towards nucleophilic attack while studying charge-transfer reactions: molecular/ ionic specimens having more or less positive *EA* values tend to behave mostly as good electron acceptor or donor respectively. Similarly, another most frequently used indicator in QSPR studies is Electronegativity (χ) as it enables to measure the tendency of attracting shared electron pair towards bonded atoms or group of atoms of the molecules or ions [38]. More explicitly, the quantum mechanically derived absolute value of it is used to pinpoint the polar region/s of the molecule: greater the *electronegativity*, stronger is the intensity of an atom or a substituent group to attract electron pairs towards it; creating oppositely charged terminals.

In quantum mechanics, all three descriptors (*IP*, *EA*,χ) are mathematically related to the DFT predicted Eigen values of the HOMO and LUMO: E_{HOMO} and E_{LUMO} (Eqs.1-3). The absolute numerical values of them (eV) for the variably sized hydrated sulfate clusters $[SO_4(H_2O)_n]^{2-}$, n = 1-4 &16 are summarized in Table 1. While comparing the magnitude of the IP for $[SO_4(H_2O)_n]^{2-}$, n = 1-4 clusters, the order is: $[SO_4(H_2O)]^{2-} > [SO_4(H_2O)_2]^{2-} > [SO_4(H_2O)_3]^{2-} > [SO_4(H_2O)_4]^{2-}$. It means, among these clusters, the last ion with $n = 4$ has more propensity to loose electrons or to generate its cationic form than with other hydrated ions. It further suggests that $[SO_4(H_2O)_4]^{2-}$ ion has less tightly held but more polarizable type electron cloud than with other ions and so on. This is quite reasonable because the electrons of its centrally located sulfate ion are decentralized/ delocalized to four surrounding H_2O molecules symmetrically as confirmed by the same author elsewhere quantum mechanically [20]. Similarly, an order of the same ionic clusters in terms of their *EA* values (magnitude) is decreasing: $[SO_4(H_2O)]^{2-} > [SO_4(H_2O)_2]^{2-} > [SO_4(H_2O)_3]^{2-} > [SO_4(H_2O)_4]^{2-}$, implying that the first ion can accept the electron more readily (good electron acceptor) than that by any other ions. Alternatively, a relatively smaller magnitude of the *EA* for the $[SO_4(H_2O)_4]^{2-}$ ion signifies the absence of strongly nucleus-pulled electron cloud which actually makes this ion to give up its electrons more facilely. Such quantum mechanically predicted high electron-accepting property of the $[SO_4(H_2O)]^{2-}$ and $[SO_4(H_2O)_2]^{2-}$ ions could support the fact "$[SO_4(H_2O)]^{2-}$ and $[SO_4(H_2O)_2]^{2-}$ ions hardly exist in the aqueous type solutions and hence, always have high preference of undergoing more sequential hydration (gaining H_2O molecules: $[SO_4(H_2O)n_{-1}]^{2-} + H_2O \rightarrow [SO_4(H_2O)n]^{2-}$) through intensive distribution of atomic charges from the central SO_4^{2-} unit to nearby hydrated H_2O molecules". A more genuine yet quite supportive explanation for the *IP*, *EA*, and χ predicted electronic polarizabilities and the electronic rigidness is presented in the following subsection 3.2.2 on the basis of DFT derived numeral values of chemical hardness (η) and chemical softness (σ).

Table 1. The DFT computed quantum chemical descriptors (QCDs) of variably sized hydrated sulfate clusters $[SO_4(H_2O)_n]^{2-}$, n = 1-4 & 16.

	Hydrated sulfate ions				
QCDs (eV)	**$[SO_4(H_2O)]^{2-}$**	**$[SO_4(H_2O)_2]^{2-}$**	**$[SO_4(H_2O)_3]^{2-}$**	**$[SO_4(H_2O)_4]^{2-}$**	**$[SO_4(H_2O)_{16}]^{2-}$**
E_{HOMO}	4.218	3.189	2.527	1.737	4.364
E_{LUMO}	13.200	12.122	11.090	10.275	7.413
ΔE_{gap}	8.98	8.93	8.56	8.54	3.05
IP	– 4.218	–3.189	–2.527	–1.737	–4.364
EA	–13.200	–12.122	–11.090	–10.275	–7.413
χ	– 8.71	–7.65	–6.81	–6.01	–5.89
η	4.49	4.46	4.32	4.27	1.52
σ	0.223	0.224	0.231	0.234	0.658
μ	8.71	7.65	6.81	6.01	5.89
ω	8.45	6.56	5.37	4.23	11.41

3.2.2 Chemical Hardness (η) and Softness (σ)

In order to explain the stability of the transition metal complexes and the mechanism of their chemical reactions, R. G. Pearson had introduced a qualitative concept for Hard and Soft Acids and Bases (HSAB principle) in 1963. However, the same concept was realized as a fundamental tool to characterize and classify Lewis acids and Lewis bases type molecular compounds into hard or soft or borderline types on the basis of frontier molecular orbital (FMO) analysis using HOMO-LUMO interactions. In general, FMO analysis states that the Lewis acid-base type interactions are mainly controlled by the relative energies E of the participating FMOs: HOMO (E_{HOMO}) & LUMO (E_{LUMO}), and the energy gap (ΔE) between them. The closely related terminologies of the Hard and Soft category of Lewis acids and Lewis bases that are responsible to quantize the electronic polarizability of the interacting chemical species are chemical hardness (η) and chemical softness (σ) respectively. Literally, the term "Hard" refers to those chemical species that are characterized by high charge density, small ionic size, non-polarizable electron cloud, and high preference of participation in ionic bonding interactions whereas "Soft" applies to those which have low charge density and are large and strongly polarizable [39]. The quantitative prediction of these structure based properties through quantum mechanical descriptors η, and σ enable chemists/physicists to understand kinetic stabilities or chemical reactivities of any molecular/ionic species without referring to large supercomputers and databases. As formulated in Eqs. 4 and 5 in introduction section, these electronic descriptors representing respectively for "Hard" and "Soft" characteristics are mathematically related to molecular orbital based quantitative parameters E_{HOMO}, E_{LUMO}, and ΔE_{gap}. Within the range of DFT computational scheme, η is defined as the second order derivative of the electronic energy E of a chemical/ionic system with respect to number of electrons N, for a fixed external potential $V(r)$: $\eta = \frac{1}{2}\left[\frac{\partial^2 E}{\partial N^2}\right] = \frac{1}{2}[\frac{\partial \mu}{\partial N}]$, and σ is an inverse of η. Thus, in broader sense, both σ and η measures how intensely the molecular/ionic specimens acquire electrons, and hence describes their chemical reactivity or kinetic stability quantitatively. While correlating these descriptors with the HOMO-LUMO energy gap ΔE_{gap} (Figure 1-Figure 5), it can be deduced that smaller (larger) the η (σ) value easier is the electronic transition from HOMO to LUMO implying that more reactive the molecular specimens become. In a reverse way, those molecular/ionic specimens which possess larger (smaller) ΔE_{gap} always have high (low) degree of hardness, and hence become less (more) reactive or hard (soft) specimens. Again, molecules/ions having lower ΔE_{gap} always have easier electronic polarization, stressing that the molecular/ionic hardness has a closed relation with electronic polarizability. Moreover, on the basis of ΔE_{gap}, the fundamental concept of "Activation Hardness" can also be defined and used more especially in differentiating the rates of the reactions occurred at different reactive sites of the molecule, and hence it is more appropriate while predicting orientation effects as well.

The mathematically derived absolute values of the η and σ descriptors for the variably sized hydrated sulfate clusters $[SO_4(H_2O)_n]^{2-}$, n = 1-4 & 16 are listed in Table 1. While comparing η or σ values of these hydrated clusters, one may conclude that greater the hydration number n of the sulfate ion, lesser (greater) is the degree of chemical hardness (softness). More particularly, the biggest hydrated sulfate ion cluster $[SO_4(H_2O)_{16}]^{2-}$ sampled in this study has comparatively the lowest value of η = 1.52 *eV* (highest value of σ = 0.658), indicating this ion has the least (most) degree of chemical hardness (softness) and thus, becomes relatively most reactive or least kinetically stable with more significant electronic polarizability. Similarly, η and σ are almost identical in magnitudes among the clusters with n = 1 to 4 further suggesting that they must have quite comparable chemical reactivities or kinetic stabilities. In terms of electronic polarizability, the relatively hardest and the least reactive $[SO_4(H_2O)]^{2-}$ ion must have restricted electronic polarizations due to the presence of tightly-held electron cloud than in the $[SO_4(H_2O)_2]^{2-}$, $[SO_4(H_2O)_3]^{2-}$, and $[SO_4(H_2O)_4]^{2-}$ ions which must have relatively easily, more easily, and the most easily polarizable electron clouds respectively, further making them to be characterized as a relatively soft, softer and the softest hydrated sulfate ion respectively. Such a weak inbound electronic cloud or firmness, and the most electronic polarizability characteristics of the $[SO_4(H_2O)_4]^{2-}$ hydrated state makes itself to loose electron comparatively most easily, *i.e.*, it should have the lowest magnitude of *IP* as predicted by the DFT (Table 1: more logical interpretations behind it are already explained in subsection 3.2.1). Energetically, $[SO_4(H_2O)_{16}]^{2-}$ state is relatively more stable than other clusters with n = 1, 2, 3, 4; $[SO_4(H_2O)_4]^{2-}$ state is relatively less stable than other bigger clusters but more stable than smaller clusters and so on; and the same is their order of thermodynamic stability ($[SO_4(H_2O)_{16}]^{2-}$ > $[SO_4^{2-}(H_2O)_4]^{2-}$ > $[SO_4^{2-}(H_2O)_3]^{2-}$ > $[SO_4^{2-}(H_2O)_2]^{2-}$ > $[SO_4^{2-}(H_2O)]^{2-}$) as well [6], but in terms of tendencies of their HOMO electrons to initiate the particular charge transfer events or chemical reactions (HOMO to LUMO transition event), the kinetic stability order of them is predicted as just opposite: $[SO_4(H_2O)_{16}]^{2-}$ (ΔE = 3.05 eV) < $[SO_4(H_2O)_4]^{2-}$ (ΔE = 8.54 eV) < $[SO_4(H_2O)_3]^{2-}$ (ΔE = 8.56 eV) < $[SO_4(H_2O)_2]^{2-}$ (ΔE = 8.93 eV) < $[SO_4(H_2O)]^{2-}$ (ΔE = 8.98 eV) because the HOMO electrons are considered as the most reactive electrons, and their rapid transition to LUMO (due to less HOMO–LUMO energy gap) determines ionic/molecular kinetic stability or reactivity quantum mechanically.

3.2.3 Electronic chemical potential (μ) and Electrophilicity index (ω)

As like as chemical-hardness (η), the DFT derived electronic chemical potential (μ) is also extremely useful to predict structure based properties in QSPR studies. In terms of working principle, the first indicator is used to measure how intensely the molecular/ionic specimens acquire electrons whereas the second indicator is used to measure escaping tendency of the electronic cloud from one ionic/molecular specimen to another when they combine mutually in the ground electronic state conditions [40]. The net electronic chemical potential (μ) actually arises whenever two reacting specimens 'X' and 'Y' have unidentical electron density fleeing propensity. For example, if μ_X represents electronic chemical potential for 'X' and $\mu_Y$is that for 'Y', and if $\mu_X > \mu_Y$, the electronic cloud from 'X' fluxes towards 'Y' until the interacting chemical system achieves the equilibrated electronic chemical potential μ_{XY}. In this case, the specimen 'X' behaves as electron-donor or nucleophile and 'Y' as electron-acceptor or electrophile and a difference in their chemical potentials $\Delta\mu$ ($\mu_X - \mu_Y$) approximates the extent of global electron density transfer (GEDT) in polar chemical reactions [41]. Quantum mechanically, μ is equal to negative of the electronegativity (χ) in Mulliken and Pauling scale (Eq. (6)). The physical meaning of it can be extended to interpret electronic polarizability of the interacting molecular/ionic specimens: lower the magnitude of μ, more easy is to gain an electron (instead, more difficult is to lose) or more firmly the electron cloud is centralized around the molecular/ionic specimens.

Similarly, Parr *et al.* [42] has defined Electrophilicity index (ω) as an effective quantum-mechanical indicator that can measure energy lowering associated with an occurrence of utmost electron flow from the donor to acceptor species. It actually quantifies the electron acceptor propensity to gain an additional electronic charge from the interacting molecular/ionic specimen [43] and hence, estimates the electron-loving or electrophilic tendency of the molecular or ionic specimens. This unique characteristic feature of ω makes itself one of the most important indicator in electrophile-nucleophile chemistry while analyzing electrophilicity of the majority of the interacting organic specimens and their chemical reactions. From the quantum mechanical viewpoint, it is defined mathematically by Eq. (7) where a direct relation of it with square of the chemical potential (μ^2), and inverse relation of it with chemical hardness (η) are formulated. This relationship is used to identify the most effective electrophile: those molecular or ionic specimens having higher value of μ^2, but lower value of η must have relatively higher value of ω, specifying such particular specimens as most electron-loving species.

The theoretically determined values of η and ω for the variably sized hydrated sulfate ion clusters $[SO_4(H_2O)_n]^{2-}$, n =1-4 &16 are listed in Table 1. The relatively higher values of μ, and ω but comparable value of η for $[SO_4(H_2O)]^{2-}$ ion ($\mu = 8.71eV$, $\omega = 8.45\ eV$, $\eta = 4.49\ eV$) than that for bigger clusters with n = 2, 3 & 4 indicates that the first ion has a high degree of electrophilicity or strong electrophilic character (difficult (easy) to lose (gain) electron, and presence of tightly-held electron cloud) than the latter ions and accordingly, the last ion with n = 4; $[SO_4(H_2O)_4]^{2-}$ ($\mu = 6.01\ eV$, $\omega = 4.23\ eV$, $\eta = 4.27\ eV$) has the least degree of electron loving tendency among them due to its relatively more polarizable and less strongly-held electron cloud as explained above in subsection 3.2.2. In the case of $[SO_4(H_2O)_{16}]^{2-}$ ion ($\mu = 5.89\ eV$, $\omega = 11.41\ eV$, $\eta = 1.52\ eV$), the degree of chemical hardness is relatively low indicating this particular ion is comparatively more reactive and has less firmly held electron cloud (more polarizable electron density) plus weak electrophilic character. As a whole, all these hydrated clusters may show high preference towards accepting electron pair from the nucleophile such as H_2O (the lone pairs on the central O atom in H_2O can be donated readily to form a bond) illustrating the possibility of forming more and more bigger hydrated clusters step-by-step through this addition type reaction: $[SO_4(H_2O)n_{-1}]^{2-} + H_2O \rightarrow [SO_4(H_2O)n]^{2-}$. Moreover, the charge separation reaction of the SO_4^{2-} ion ($[SO_4(H_2O)n]^{2-} \rightarrow [HSO_4(H_2O)n_{-k}]^{-} + [OH(H_2O)_{k-1}]^{-}$) transforming into HSO_4^- and OH^- is governed by the variation in their hydration strength: the reactant SO_4^{2-} and the product OH^- interact with H_2O relatively stronger than HSO_4^- ion [44]. It is reported elsewhere [44] that the reaction barrier is relatively higher whenever >2H_2O molecules are left from the reactant $[SO_4(H_2O)n]^{2-}$ to hydrate the products HSO_4^- and OH^-, and such charge separation propensity is relatively higher in the clusters with n = 3 and 4 (e.g. $[SO_4(H_2O)_4]^{2-} \rightarrow [HSO_4(H_2O)]^{-} + [OH(H_2O)_2]^{-}$), however in the clusters with $n > 6$ and other relatively larger clusters, the charge separation is dominated by dissociation *via* loss of H_2O molecule. In the case of $[SO_4(H_2O)_4]^{2-}$ cluster, this charge separation reaction is favored by an intermediate represented by the hydrogen bond bound ($[HSO_4(H_2O)]^-$ & $[OH(H_2O)_2]^-$) products followed by the columbic repulsion between these anions whereas in the bigger clusters, loss of H_2O is preferred due to the existence of weak hydrogen bond between central SO_4^{2-} unit and the outersphered H_2O molecules (the innersphered H_2O molecules screen the inward binding force of the outersphered H_2O) plus higher stability of the resulting products in hydrated states. It is supported here as well that the symmetric cluster $[SO_4(H_2O)_4]^{2-}$ ($\mu = 6.01\ eV$, $\omega = 4.23\ eV$, $\eta = 4.27\ eV$) has more polarizable electron cloud which actually enhances this ion to lose or dissociate H_2O leading to the formation of charge-separated products, and the biggest cluster $[SO_4(H_2O)_{16}]^{2-}$ ($\mu = 5.89\ eV$, $\omega = 11.41\ eV$, $\eta = 1.52\ eV$) sampled in this study is chemically softest and hence, may show more affinity towards taking part in chemical reactions either by losing H_2O molecules (dissociation of the cluster) to the environment or by exchanging them between inner and outer solvation shells (average time an ion spends in a hydration shell (~ 2-4 nanoseconds) is about two orders of magnitude longer than the lifetime of an individual H_2O–H_2O hydrogen bond [45]).

To predict the degree of GEDT between any two pre-selected sulfate ionic pairs, the concerned $\Delta\mu$ values are calculated, and the extent of transferring electron density flux is speculated. For example, the significantly low $\Delta\mu$ ($\Delta\mu = \mu_1 - \mu_2$) values for the ionic pairs: (1) $[SO_4(H_2O)]^{2-}$ and $[SO_4(H_2O)_2]^{2-}$ ($\Delta\mu$ = 1.06 eV), (2) $[SO_4(H_2O)_2]^{2-}$ and $[SO_4(H_2O)_3]^{2-}$ ($\Delta\mu$ = 0.84 eV), and (3) $[SO_4(H_2O)_3]^{2-}$ and $[SO_4(H_2O)_4]^{2-}$ ($\Delta\mu$ = 0.80 eV) confirm that the GEDT between them is relatively small. These data eventually tells us that the rate of transferring electron density flux between these ionic pairs is in the order [$[SO_4(H_2O)]^{2-}$ to $[SO_4(H_2O)_2]^{2-}$] > [$[SO_4(H_2O)_2]^{2-}$ to $[SO_4(H_2O)_3]^{2-}$] > [$[SO_4(H_2O)_3]^{2-}$ to $[SO_4(H_2O)_4]^{2-}$]. Therefore, the unanimous conclusion one can draw here is these ionic pairs must have some chances of occurring electron/ charge transfer events [46] even though more trustworthy experimental and theoretical results are required.

IV. CONCLUSION

In molecular modeling and structure entry steps of computational chemistry and chemical drug design, predicting the most significant physicochemical properties of the molecules simply on the basis of knowledge of their three dimensional structures (Quantitative Structure-Property Relationships Approach: QSPR) plays vital role. In addition to it, the same structure-property correlation feature of this predictive molecular based approach is regarded as quite significant more especially in revealing chemical reactivities or kinetic stabilities of the molecular/ionic specimens quantitatively. In this study, the global quantum-chemical reactivity descriptors (QCDs) that are directly derivable from the DFT produced electron density based 3D molecular structure such as energy of the HOMO (E_{HOMO}) and LUMO (E_{HOMO}), HOMO–LUMO energy gaps (ΔE_{gap}), ionization potential (IP), electron affinity (EA), chemical hardness (η), chemical softness (σ), electronic chemical potential (μ), electrophilicity index (ω), and electronegativity (χ) are chosen, and on the basis of their absolute numerical values, the QSPR analyses including relative chemical or kinetic stabilities of variably sized hydrated sulfate ion clusters $[SO_4(H_2O)_n]^{2-}$, n = 1-4 & 16 are explored quantum mechanically.

Prior to determine the absolute values of those QCDs involved in this QSPR studies for $[SO_4(H_2O)_n]^{2-}$, n = 1-4 & 16, the DFT computed surface plots of their individual frontier molecular orbitals were thoroughly analyzed, and observed that HOMO is the highest occupied, non-bonding, and highly localized electron density surface present around centrally located SO_4^{2-} unit while LUMO is the lowest unoccupied orbital surface displaying significant probability electron density over centrally inbound but peripheral H_2O molecules. The HOMO and LUMO energy extracted from the DFT generated quantum mechanical information, and their gaps ΔE_{gap} calculated as $\Delta E_1 = 8.98\, eV$, $\Delta E_2 = 8.93\, eV$, $\Delta E_3 = 8.56\, eV$, $\Delta E_4 = 8.54\, eV$,and $\Delta E_5 = 3.05\, eV$ respectively for $[SO_4(H_2O)_n]^{2-}$, n = 1-4 &16 hydrated states were found not only to approximate their electronic band gaps but also to imprecise their lowest energy transition frequency in UV visible spectroscopy. On the basis of same ΔE_{gap} values, the mathematical indices for all the DFT based QCDS (*IP*, *EA*,η, σ, μ, and ω) were determined for each of these hydrated sulfate clusters, and the concerned 3D structure-property correlations were interpreted quantitatively. The relatively smaller magnitude of *IP* and *EA* showed that $[SO_4(H_2O)_4]^{2-}$ cluster has more propensity to loose electrons or to generate its cationic form and has less tightly held (nucleus-pulled) or more polarizable type electron cloud than in other hydrated ions with $n < 4$. Similarly, the comparatively lowest value of η (η = 1.52 *eV*) but highest value of σ (σ = 0.658) marked $[SO_4(H_2O)_{16}]^{2-}$ ionic cluster as the most reactive (least (most) degree of chemical hardness (softness)) or less kinetically stable with more significant electronic polarizability among other smaller clusters sampled in this study. Moreover, among the ions with $n \leq 4$, the calculated values of μ, and ω predicted $[SO_4(H_2O)_4]^{2-}$ ($\mu = 6.01\, eV$, $\omega = 4.23\, eV$) cluster under that type which has the least degree of electron loving tendency and accordingly, the biggest hydrated sulfate cluster $[SO_4(H_2O)_{16}]^{2-}$ ($\mu = 5.89\, eV$, $\omega = 11.41\, eV$, $\eta = 1.52\, eV$) sampled in this study was also marked as an ion having a significantly weak electrophilic character.

Even though all the DFT derived HOMO and LUMO Eigen values and their band gaps(ΔE_{gap}) plus the mathematically determined values of the QCDs for the variably sized hydrated sulfate ion clusters would be as reliable as those obtained through high-level computational methods, this QSPR study was mainly limited to computationally cheap hybrid density functional DFT: B3LYP with 6–31G (*d*, *p*) basis set due to the shortage of enough computational resources. One may use more advanced theoretical models with systematically convergent basis sets for explicitly correlated wave functions [47] to reinforce the results reported here

REFERENCES

[1] M. Karelson, V. S. Lobanov, A. R. Katritzky, "Quantum-Chemical Descriptors in QSAR/ QSPR Studies", *Chemical Review*, Vol. **96 (3)**, pp. **1027–1043**, **1996**.

[2] Peixun Liu, Wei Long, "Current Mathematical Methods Used in QSAR/QSPR Studies", *International Journal of Molecular Sciences*, Vol. **10(5)**, pp. **1978–1998**, **2009**.

[3] J. Fei, Q. Mao, L. Peng, T. Ye, Y. Yang, S. Luo, "The Internal Relation between Quantum Chemical Descriptors and Empirical Constants of Polychlorinated Compounds", *Molecules*, Vol. **23(11)**, pp. **2935:1–12**, **2018**.

[4] J. Jaworska, N. Nikolova-Jeliazkova, T. Aldenberg, "QSAR applicability domain estimation by projection of the training set in descriptor space: A review", *Alternatives to Laboratory Animals*, Vol. **33**, pp. **445–459**, **2005**.

[5] T. Papp, L. Kollar, T. Kegl, "Employment of quantum chemical descriptors for Hammett constants: Revision Suggested for the acetoxy substituent", *Chemical Physics Letter*, Vol. **588**, pp. **51–56**, **2013**.

[6] W. L. Jolly, "Modern Inorganic Chemistry", McGraw-Hill Book Company, New York, **1984**.

[7] E. C. Koch, "Acid-Base Interactions in Energetic Materials: "I. The Hard and Soft Acids and Bases (HSAB) Principle-Insights to Reactivity and Sensitivity of Energetic Materials", *Propellants, Explosives, Pyrotechnics*, Vol. **30(1)**, pp. **5–16**, **2005**.

[8] M. S. A. Abdel–Mottaleb, S. N. Ali, "A New Approach for Studying Bond Rupture/Closure of a Spiro Benzopyran Photochromic Material: Reactivity Descriptors Derived from Frontier Orbitals and DFT Computed Electrostatic Potential Energy Surface Maps", *International Journal of Photoenergy*, Article ID **6765805**, pp. **1–9**, **2016**.

[9] S. Kumar, A. Syed, S. Andotra, R. Kaur, Vikas, S. K. Pandey, "Investigation of synthesized new vanadium(III) complexes of ditolyldithiophosphate ligands by spectroscopic, cyclic voltammetric, DFT, antimicrobial and cytotoxic studies", *Journal of Molecular Structure*, Vol. **1154**, pp. **165–178**, **2018**.

[10] M. Saranya, S. Ayyappan, R. Nithya, R. K. Sangeetha, A. Gokila, "Molecular structure, NBO and HOMO–LUMO analysis of quercetin on single layer graphene by density functional theory", *Digest Journal of Nanomaterials and Biostructures*, Vol. **13**, No. **1**, pp. **97–105**, **2018**.

[11] T. Abbaz, A. Bendjeddou, D. Villemin, "Molecular orbital studies (hardness, chemical potential, electro negativity and electrophilicity) of TTFs conjugated between 1, 3–dithiole", *International Journal of Advanced Research in Science, Engineering and Technology*, Vol. **5(2)**, pp. **5150–5161**, **2018**.

[12] T. M. Nolte, W. J. G. M. Peijnenburg, "Use of quantum-chemical descriptors to analyse reaction rate constants between organic chemicals and superoxide/hydroperoxyl ($O_2^{\bullet-}$/$HO_2^{\bullet}$)", *Free Radical Research*, Vol. **52(10)**, pp. **1118–1131**, **2018**.

[13] P. Hohenberg, W. Kohn, "Inhomogeneous Electron Gas", *Physical Review B*, Vol. **136**, No. **3B**, pp. **864–871**, **1964**.

[14] W. Kohn, L. Sham, "Self-Consistent Equations Including Exchange and Correlation Effects", *Physical Review Journal*", Vol. **140**, No. **4A**, pp. **A1133–A1138, 1965**.

[15] A. B. Marahatta, "A DFT Analysis for the Electronic Structure, Mulliken Charges Distribution and Frontier Molecular Orbitals of Monolayer Graphene Sheet", *International Journal of Progressive Sciences and Technologies*, Vol. **16**, No. **1**, pp. **51–65**, **2019**.

[16] A. B. Marahatta, "Effect of n-Type Dopant Nitrogen in the Structure and Atomic Charges Distribution of Monolayer Graphene Sheet: A DFT Analysis", *International Journal of Progressive Sciences and Technologies*, Vol. **16**, No. **2**, pp. **01–13**, **2019**.

[17] A. B. Marahatta, "DFT Study on Ground State Electronic Structures of Simple to Complex Molecular Specimens", *International Journal of Progressive Sciences and Technologies*, Vol. **19**, No. **1**, pp. **100–112**, **2020**.

[18] A. B. Marahatta, H. Kono, "Comparative Theoretical Study on the Electronic Structures of the Isolated Molecular Gyroscopes with Polar and Nonpolar Phenylene Rotator", *International Journal of Progressive Sciences and Technologies*, Vol. **20**, No. **1**, pp. **109–122**, **2020**.

[19] A. B. Marahatta, "Computational Study on Electronic Structure, Atomic Charges Distribution and Frontier Molecular Orbitals of Butadiene: General Features for Diels-Alder Reaction", *International Journal of Progressive Sciences and Technologies*, Vol. **19**, No. **2**, pp. **48–64**, **2020**.

[20] A. B. Marahatta, "A DFT Study of Electronic Structures on Hydrated Sulfate Clusters $[SO_4^{2-}(H_2O)_n]$" n = 0–4,16", *International Journal of Progressive Sciences and Technologies*, Vol. **17**, No. **1**, pp. **55–69**, **2019**.

[21] A. B. Marahatta, "Theoretical Study on Microhydration of Bisulfate Ions $[HSO_4^{-}(H_2O)_n]$" n = 0–3, 5", *International Journal of Progressive Sciences and Technologies*, Vol. **18**, No. **2**, pp. **43–53**, **2020**.

[22] R. G. Parr, Y. Weitao, "*Density-Functional theory of Atoms and Molecules*", Oxford University Press, **1994**.

[23] L. R. Domingo, M. Ríos-Gutiérrez, P. Pérez, "Applications of the Conceptual Density Functional Theory Indices to Organic Chemistry Reactivity", *Molecules*, Vol. **21(748)**, pp. **1–22**, **2016**.

[24] A. B. Marahatta, "DFT Study on Electronic Charge Distribution and Quantum-Chemical Descriptors for the Kinetic Stability of Vanadium Aquo Complex Ions $[V(H_2O)_6]^{2+}$ and $[V(H_2O)_6]^{3+}$", *International Journal of Progressive Sciences and Technologies*, Vol. **22**, No. 1, pp. **67–81**, **2020**.

[25] A. T. Blades and P. Kebarle, "Sequential Hydration Energies of the Sulfate Ion, from Determinations of the Equilibrium Constants for the Gas-Phase Reactions: $SO_4(H_2O)_n^{2-} = SO_4(H_2O)_{n-1}^{2-} + H_2O$", *Journal of Physical Chemistry A*, Vol. **109(37)**, pp. **8293–8298**, **2005**.

[26] D. Markovich, "Physiological Roles and Regulation of Mammalian Sulfate Transporters", *Physiological Reviews*, Vol. **81(4),** pp. **1499–2021**, **2001**.

[27] M. Jung, W. Lee, C. Noh, A. Konovalova, G. S. Yi, S. Kim, Y. Kwon, D. Henkensmeier, "Blending polybenzimidazole with an anion exchange polymer increases the efficiency of vanadium redox flow batteries", *Journal of Membrane Science*, Vol. **580**, pp. **110–116**, **2019**.

[28] D. Pavlov, "*Lead Acid Batteries: Science and Technology"*, Elsevier publication, **2011**.

[29] Food and Nutrition Board, Institute of Medicine of the National Academies, "*Dietary Reference Intakes for Water, Potassium, Sodium, Chloride, and Sulfate*", National academic press, **2005**.

[30] *Sodium Sulfate Functions in Daily Life–Formula–Uses*, https://azchemistry.com/sodium-sulfate-function.

[31] Æ. Frisch, H. P. Hratchian, R. D. Dennington II, T. A. Keith, J. Millam, "*Gauss view 05 Reference*", Gaussian, Inc., **2009**.

[32] L. C. Smeeton, J. D. Farrell, M. T. Oakley, D. J. Wales, R. L. Johnston, "Structures and Energy Landscapes of Hydrated Sulfate Clusters", *Journal of Chemical Theory and Computation*, Vol. **11(5)**, pp. **2377–2384**, **2015**.

[33] *Gaussian 09 manual*, *http://gaussian.com/geom/?tabid=1#GeomkeywordReadOptimi zeoption*

[34] Æ. Frisch, "Gaussian 09W Reference", Gaussian, Inc., **2009**.

[35] Reenu, Vikas, "Exploring the role of quantum chemical descriptors in modeling acute toxicity of diverse chemicals to Daphnia magna Bajorath", *Journal of Molecular Graphics and Modelling,* Vol. **61**, pp. **89–101**, **2015**.

[36] *Quantitative Structure Activity Relationship*. In: Schwab M. (ed) Encyclopedia of Cancer, Springer, Berlin, **2011**.

[37] G. Parr, R. G. Pearson, "Absolute hardness: companion parameter to absolute electronegativity", *Journal of American Chemical Society*, Vol. **105(26)**, pp. **7512–7516**, **1983**.

[38] W. L. Jolly, "Modern Inorganic Chemistry", McGraw-Hill Book Company, New York, **1984**.

[39] E. C. Koch, "Acid-Base Interactions in Energetic Materials: I. The Hard and Soft Acids and Bases (HSAB) Principle-Insights to Reactivity and Sensitivity of Energetic Materials", *Propellants, Explosives, Pyrotechnics*, Vol. **30**(1), pp. **5–16**, **2005**.

[40] R. G. Parr, Y. Weitao, "*Density-Functional theory of Atoms and Molecules*", Oxford University Press, **1994**.

[41] L. R. Domingo, M. Ríos-Gutiérrez, P. Pérez, "Applications of the Conceptual Density Functional Theory Indices to Organic Chemistry Reactivity", *Molecules*, Vol. **21(748)**, pp. **1–22**, **2016**.

[42] R. G. Parr, L. V. Szentpály, S. Liu, "Electrophilicity Index", *Journal of American Chemical Society*, Vol. **121(9)**, pp. **1922–1924**, **1999**.

[43] H. Tandon, T. Chakraborty, V. Suhag , "A New Scale of the Electrophilicity Index Invoking the Force Concept and Its Application in Computing the Internuclear Bond Distance" *Journal of Structural Chemistry*, Vol. **60**, *pp.* **1725–1734**, **2019**.

[44] B. Gao, Z. Liu, "Size-dependent charge-separation reaction for hydrated sulfate dianion cluster, $[SO_2^{-4}(H_2O)_n]$ with n = 3–7", *The Journal of Chemical Physics*, Vol. **123**, pp. **224302**, **2005**.

[45] S. Lower, "*Chem1 General Chemistry Virtual Textbook"*, Department of Chemistry, Simon Fraser University, Burnaby/Vancouver, Canada.

[46] J. M. J. Swanson, J. Simons, "The role of charge transfer in the structure and dynamics of the hydrated proton", *Journal of Physical Chemistry B*, Vol. **113(15)**, pp. **5149–5161**, **2009**.

[47] *A. P.* Kirk, T. B. Adler**,** H. J. Werner**, "**Systematically convergent basis sets for explicitly correlated wavefunctions: The atoms H, He, B–Ne, and Al–Ar", *Journal of Chemical Physics*, Vol. **128**(8), pp. **084102**, **2008**.